ELSEVIER

Marine Geology 229 (2006) 187–198

MARINE GEOLOGY
INTERNATIONAL JOURNAL OF MARINE GEOLOGY, GEOCHEMISTRY AND GEOPHYSICS

www.elsevier.com/locate/margeo

Some remarks on the thermal nature of the double BSR

Alexander Ya. Golmshtok *, Valery A. Soloviev ✠

St. Petersburg Branch of P.P. Shirshov Institute of Oceanology, Russian Academy of Sciences, 30, Line 1, 199053 St. Petersburg, Russia

Received 29 March 2005; received in revised form 5 March 2006; accepted 14 March 2006

Abstract

The numerical solution of the heat transfer problem, which takes into account the latent heat (Stefan problem) of the gas hydrate dissociation, shows that the "double BSR" at the Nankai Trough site could have been caused by the upwards displacement of a previously deeper phase boundary (base of the gas hydrate stability zone) after an abrupt increase of the sea-bottom temperature by approximately 4 °C or more, which happened about 10 ka ago. The obtained conclusions are believed to be correct for other areas of the Ocean as well, where two or more BSRs have been observed. In order to explain the nature of the phenomenon of the "double BSR" it is necessary to examine also other factors besides paleooceanographic ones, for example, lithological–geochemical properties of sediments.

Keywords: bottom-simulating reflections; finite-difference method; gas hydrates; Stefan problem; temperature

1. Introduction

Observation of a Bottom Simulating Reflection (BSR) on seismic sections is the basic geophysical evidence of the potential presence of gas hydrates in the sedimentary section below the sea floor (Tucholke et al., 1977). Reflectors that are parallel to the sea bottom can be of different nature, for example, associated with a diagenetic boundary (opal-A to opal-KT transition; Berndt et al., 2004) or hydrate-related. A hydrate-related reflector is identified on seismic records by the following characteristics: (1) the conformity of the BSR and the sea floor with, as a rule, increase of BSR subbottom depth when the water depth increases; (2) crossing of the BSR with reflections from sedimentary sequences; (3) reversed phase of the BSR in comparison with the sea-floor reflection, and (4) commonly higher amplitude sedimentary reflections below than above. A direct indication of the BSR is its spatial correspondence with the base of gas hydrate stability zone determined from geothermal data.

It is generally accepted that the occurrence of the hydrate-related BSR is caused primarily by the presence of some quantity of free gas below the base of the hydrate stability zone (BHSZ) rather than by the presence of hydrates above. The presence of the free gas in the pore space of the sediments significantly reduces the compressional seismic velocity. This results in a negative contrast in the acoustic impedance at the considered phase boundary, and causes both the large absolute values and the negative sign of the reflection coefficient (Shipley et al., 1979). An increase of the free gas concentration in the pore space from 0% up to 1% leads to a decrease of the seismic velocity down to 1200 m/s (Domenico, 1976; Murphy, 1984). Hence, the BSR can be considered as a peculiar expanded "bright" which has no association with the

* Corresponding author. Tel.: +7 812 738 71 83.
E-mail address: golmshtok@newmail.ru (A.Ya. Golmshtok).
✠ Deceased on 2005-09-14.

0025-3227/$ - see front matter © 2006 Published by Elsevier B.V.
doi:10.1016/j.margeo.2006.03.004

structure or lithology of the sedimentary cover. The presence of the free gas phase below the BHSZ can be caused by (1) inflow of free or water-dissolved gas from below, providing oversaturation in the pore water, or by (2) displacement of the BHSZ upwards. The latter can be the result of one of the following processes: increase of sea-bottom temperature, tectonic uplift of the sea floor or intensive sedimentation.

Many existing data sets revealing BSRs testify that its characteristics may vary within the area of the site, and even along a single seismic profile. For the Peru margin site, for example, the values of the reflection coefficient of the observed BSR vary from 0 to −0.135 along a single seismic profile (Miller et al., 1991). As the gas and water system below the BSR and the hydrate system above the BSR should be in equilibrium, this implies that both the gas and hydrate concentrations vary significantly along the profile. In the strict sense, the presence of the BSR is the integral indicator of the full gas saturation of the pore water near the BHSZ. This fact allows for the use of the seismic data in revealing the BSR for the evaluation of the hydrate amounts in the marine sediments (Ginsburg and Soloviev, 1994) and for estimation of heat flow values (Yamano et al., 1982).

In recent years, two reflections subparallel to the sea bottom, but at different subbottom depths (the so-called double BSR) were observed on many seismic sections at different hydrate sites. The upper reflection is the hydrate-related BSR and coincides with the BHSZ. The lower reflection is characterized only by indirect attributes of the BSR including the inversion of the reflection phase. This type of section was collected on the continental margin to the west of Norway (Posevang and Mienert, 1999), on the continental slope of the Nankai Trough offshore Japan (Foucher et al., 2002) and on Hydrate Ridge offshore Oregon, USA (Bangs et al., 2005). A quadruple BSR along with a double BSR was identified on the northwest slope of the Black Sea (Popescu et al., 2003).

Two extended bottom simulating reflectors, BSR1 and BSR2, were traced at the Nankai Trough site over a distance of about 10 km (i.e. profile 39 of Foucher et al., 2002). It was established that the depth of the upper reflector (BSR1) corresponds to the present-day position of the base of the methane hydrate stability zone, estimated from the temperature and pressure conditions at the ocean floor and in the sedimentary cover assuming a thermal gradient there is 35 °C/km down to this reflector. Foucher et al. (2002) hypothetically consider the lower BSR (BSR2) as a residual BSR from a former position of the BHSZ, which subsequently at some later time must have migrated to the present-day position of BSR1. They suggested that the displacement can be explained either by a pressure decrease due to 90 m tectonic uplift of the sea floor, or by an abrupt heating of the sea floor by 1–2 °C, associated with the fast warming of the upper and intermediate water layers due to horizontal migration of the Kuroshio. At the same time, the contrast of acoustic impedances at BSR2, caused by the presence of free gas below this boundary, was preserved. This contrast is sufficient for the creation of seismic reflections with inverse polarity.

The difference in depth for BSR2 and BSR1 was estimated by Foucher et al. (2002) to be equal to the displacement that would result from an increase in bottom-water temperature of 1.5 °C, about 10 ka ago. The hydrate dissociation which causes such a displacement is an endothermic reaction. It is known that the latent heat of hydrate formation is almost twice as large as that of ice formation and that it consequently significantly influences the reaction rate. Calculations, performed for other regions (Selim and Sloan, 1990; Taylor et al., 2002; Golmshtok, 2003; Sultan et al., 2004), indicated that the latent heat of gas hydrate dissociation may be the main factor determining the amount of phase boundary displacement.

In this paper we will analyze in more detail the thermal aspects of the double BSR in the Nankai Trough on the basis of the solution of the phase transition problem under the suggested bottom water temperature jump.

2. Thermal model

The model of phase boundary displacement caused by the change of sea bottom temperature that we want to apply for the Nankai Trough can be described as follows.

At 10 ka ago (this moment is considered as time zero $t=0$) the base of the methane hydrate stability zone was located at the depth $z=h_g$ (z is measured downwards from the sea floor). This depth corresponds to the depth of the BSR2 at some point of profile 39 of Foucher et al. (2002). The sediment section is represented by three layers (Fig. 1) according to most drilling data, in particular from the Nankai Trough (Matsumoto, 2002). The first, uppermost layer does not contain any methane hydrates and is characterized by porosity that changes with depth according to Athy's law (Athy, 1930):

$$\phi_1(z) = \phi_0 \exp(-kz),\ 0 \le z \le h_1, \quad (1)$$

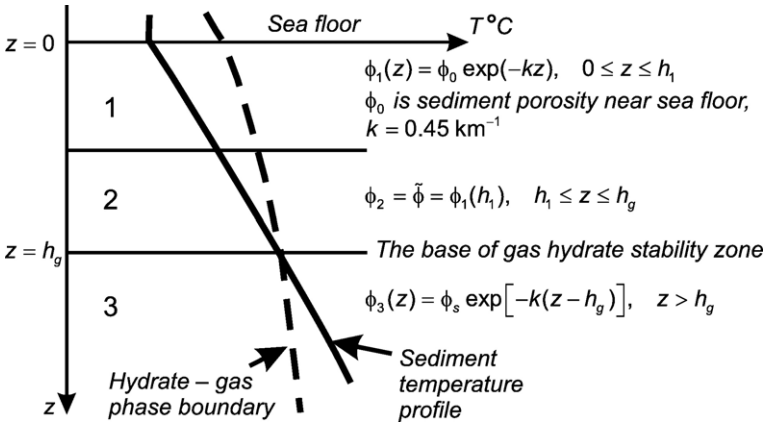

Fig. 1. Model for the geological section at the initial time. The methane hydrate bearing layer is characterized by a constant porosity, whereas in the other layers it exponentially varies with depth. At the base of the gas hydrate stability zone the sediment temperature is equal to the equilibrium temperature of hydrate dissociation.

in which $\phi_0=0.6$ is the porosity of the near sea-bottom sediments, h_1 is the thickness of the first layer, $k=4.5\cdot10^{-4}$ m^{-1} is the compaction parameter of sediments (Ozerskaya and Tuyezova, 1984).

The second layer $h_1 \le z \le h_g$ represents sediments that contain gas hydrates. It is characterized by the porosity $\phi_2(z)=\tilde{\phi}=\phi_1(h_1)$, which remains constant with depth because of the hydrate cementation.

The third layer is located below the phase boundary. Its porosity $\phi_3(z)$ changes in accordance with Athy's law, as in the first layer:

$$\phi_3(z) = \phi_s \cdot \exp(-k(z-h_g)), \quad z > h_g. \tag{2}$$

The value of the pressure-dependent porosity ϕ_s is defined by Eq. (1) for such a homogeneous medium in which the lithostatic pressure at the depth $z=h_g$ is equal to the sum of the pressures of two upper layers with porosities $\phi_1(z)$ and $\tilde{\phi}$.

We assume that prior to the warming pulse of 10 ka ago the temperature of the ocean floor was stable for a long enough period so that the thermal equilibrium in the sedimentary section could be established. In this case before the origin time ($t \le 0$) the stationary temperature $T_s(z)$ in the sedimentary strata was defined by the thermal conductivity equation:

$$\frac{d}{dz}\left[\lambda(z)\frac{dT_s(z)}{dz}\right] = 0, \tag{3}$$

where $\lambda(z)$ is the thermal conductivity of the sediments.

The temperature of the sea bottom sediments was equal to the temperature of the near-bottom water at that time:

$$T_s(z=0) = T_w^0. \tag{4}$$

The temperature of the base of the layer with methane hydrates was equal to the temperature of hydrate dissociation or the phase temperature (ph):

$$T_s(z=h_g) = T_{ph}^0. \tag{5}$$

The solution of the Eq. (3) with the boundary conditions (4) and (5) is:

$$T_s(z) = \begin{cases} T_w^0 + q_s \int_0^z dx/\lambda(x), & 0 \le z \le h_1, \\ T_{ph}^0 - \dfrac{q_s}{\tilde{\lambda}_2}(h_g - z), & h_1 \le z \le h_g, \\ T_{ph}^0 + q_s \int_{h_g}^z dx/\lambda(x), & z \ge h_g, \end{cases} \tag{6}$$

where q_s is the stationary heat flow determined by equation:

$$q_s = \frac{\tilde{\lambda}_2 \cdot (T_{ph}^0 - T_w^0)}{h_g - h_1 + \tilde{\lambda}_2 \int_0^{h_1} dx/\lambda(x)}. \tag{7}$$

We use the known dependence of the thermal conductivity of the sediments on their porosity, and thus on depth z (Budiansky, 1970):

$$\lambda(\phi) = \left(-\alpha + \sqrt{\alpha^2 + 8\cdot\lambda_{mm}\cdot\lambda_w}\right)/4, \tag{8}$$

where:

$$\alpha = 3\cdot\phi\cdot(\lambda_{mm} - \lambda_w) + \lambda_w - 2\cdot\lambda_{mm}, \tag{9}$$

λ_{mm} is the thermal conductivity of the mineral matrix of the sediments, λ_w is the thermal conductivity of the pore water. We use the following average values:

λ_{mm}=2.1 W m^{-1} K^{-1} and λ_w=0.6 W m^{-1} K^{-1} (Clauser and Huenges, 1995).

In the second layer ($h_1 \le z \le h_g$) methane hydrates occupy a portion, δ, of the pore volume. In general, the thermal conductivity of methane hydrate, λ_h, is estimated in the range of 0.5 W m^{-1} K^{-1} (Sloan, 1990; Waite et al., 2002) to 2.1 W m^{-1} K^{-1} (Groisman, 1985). Here, we examine two extreme cases when thermal conductivity of the methane hydrate is equal either to the pore water conductivity or to the conductivity of the sediment mineral matrix. The thermal conductivity of the sediments in the second layer, $\tilde{\lambda}_2$, is obtained from formulas (8) and (9) by substitution of either the constant porosity $\tilde{\phi}$ (for the pore water conductivity) or the constant $(1-\delta)\,\tilde{\phi}$ (for the mineral matrix conductivity). Thus:

$$\tilde{\lambda}_2 = \begin{cases} \lambda(\tilde{\phi}), & \lambda_h = \lambda_w, \\ \lambda((1-\delta)\cdot\tilde{\phi}), & \lambda_h = \lambda_{mm}. \end{cases} \tag{10}$$

At the time instance t=0 the temperature of the sea bottom (the water depth is denoted further by h_w) suddenly increases by ΔT=1.5 °C (Foucher et al., 2002) and for the rest of the time (t>0) it is maintained constant at that temperature $T(0, t)=T_w^0+\Delta T$.

Relatively small variations of the bottom temperature with time cannot lead to violation of the methane hydrate stability conditions in near-bottom sediments. However, the temperature perturbations migrating downwards can violate these conditions near the BHSZ as the gradient of equilibrium temperature is small and even a little positive change of the temperature $T(z, t)$ is able to provoke a noticeable upwards displacement of the boundary. It results in narrowing of the methane hydrate stability zone and leads to hydrate dissociation near the initial level $z=h_g$ of the phase boundary. The dissociation reaction is endothermic, i.e. it is accompanied by heat absorption.

If the depth of the phase boundary is defined as $z=\xi(t)$, the thermal balance at this level (the Stefan condition) may be written in the form of:

$$\frac{d\xi(t)}{dt} = \frac{1}{L\cdot\rho}\left[\tilde{\lambda}_2\cdot\left.\frac{\partial T^-(z,t)}{\partial z}\right|_{z=\xi(t)-0} - \lambda_2\cdot\left.\frac{\partial T^+(z,t)}{\partial z}\right|_{z=\xi(t)+0}\right], \tag{11}$$

where: $T(z, t)=T^-(z, t)$ and $T(z, t)=T^+(z, t)$ are the temperatures in domains $0 \le z \le \xi(t)$ and $z \le \xi(t)$, respectively; L=430 kJ/kg is the latent heat of the methane hydrate dissociation (Istomin, 1999; Sultan et al., 2004); ρ is the volumetric density of the methane hydrate (the mass of methane hydrates in a unit volume of the sediment); $\lambda_2=\lambda(\tilde{\phi})$ is the thermal conductivity of the sediments in the lower second layer's part where the methane hydrate has already dissociated.

Since hydrates fill only a portion of the pore space of the sediments, the density ρ is expressed as:

$$\rho = \rho_h\cdot\delta\cdot\phi(\xi(t)), \tag{12}$$

where ρ_h=913 kg/m^3 is the density of the methane hydrate.

The differential Eq. (11) was solved numerically using the Runge–Kutta method. Thus, on each step we numerically solved the thermal conductivity equation for the functions $T^-(z, t)$ and $T^+(z, t)$, respectively:

$$\frac{\partial}{\partial z}\left[\lambda^-(z)\frac{\partial T^-(z,t)}{\partial z}\right] - \overline{\rho C^-}(z)\frac{\partial T^-(z,t)}{\partial t} = 0, \quad 0 \le z \le \xi(t), \tag{13}$$

$$\frac{\partial}{\partial z}\left[\lambda^+(z)\frac{\partial T^+(z,t)}{\partial z}\right] - \overline{\rho C^+}(z)\frac{\partial T^+(z,t)}{\partial t} = 0, \quad \xi(t) \le z \le H, \tag{14}$$

with the boundary conditions:

$$T^-(0,t) = T_w^0 + \Delta T, \quad t > 0, \tag{15}$$

$$T^-(\xi(t),t) = T^+(\xi(t),t) = T_{ph}(\xi(t)), \tag{16}$$

$$T^+(H,t) = T_s(H), \tag{17}$$

and initial condition:

$$T(z,0) = T_s(z), \quad 0 \le z \le H, \tag{18}$$

Here: $T_{ph}(\xi(t))$ is the phase transformation temperature (at the time of t) determined using the software written by E. Sloan (Sloan, 1996) for pure methane and sea water (35‰ NaCl) in the pore space of the sediments, $\overline{\rho C}$ is the specific heat of the sediments and H is the depth at which the temperature perturbation does not exceed 0.001 °C. This depth was estimated using the known solution for the thermal problem for homogeneous half-space where the surface temperature is abruptly changed. For this case we used average values (in the range $0 \le z \le H$) of thermal conductivity and specific heat.

The values for the thermal conductivities $\lambda^{-}(z)$ and $\lambda^{+}(z)$ are defined as:

$$\lambda^{-}(z) = \begin{cases} \lambda(\phi_1(z)), & 0 \le z \le h_1, \\ \tilde{\lambda}_2, & h_1 < z \le \xi(t), \end{cases} \tag{19}$$

$$\lambda^{+}(z) = \begin{cases} \lambda_2, & \xi(t) < z \le h_g, \\ \lambda(\phi_3(z)), & z > h_g. \end{cases} \tag{20}$$

The specific heat of the sea water is equal to $\rho_w C_w = 4.18 \cdot 10^6$ J m^{-3} K^{-1} whereas for the mineral matrix it is $\rho_{mm} C_{mm} \approx (2.6\text{–}2.7) \cdot 10^6$ J m^{-3} K^{-1}. The specific heat of the methane hydrate, $\rho_h C_h$, differs slightly from similar values for the mineral matrix of terrigenous sediments (Groisman, 1985; Sultan et al., 2004). It means that the expressions for the specific heat $\overline{\rho C^{-}}(z)$ and $\overline{\rho C^{+}}$ can be written as:

$$\overline{\rho C^{-}}(z) = \begin{cases} \rho_w C_w \phi_1(z) + \rho_{mm} C_{mm}[1-\phi_1(z)], & 0 \le z \le h_1 \\ \rho_w C_w (1-\delta) \cdot \tilde{\phi} + \rho_{mm} C_{mm}[1-(1-\delta) \cdot \tilde{\phi}], & h_1 < z \le \xi(t), \end{cases} \tag{21}$$

$$\overline{\rho C^{+}}(z) = \begin{cases} \rho_w C_w \tilde{\phi} + \rho_{mm} C_{mm}(1-\tilde{\phi}), & \xi(t) < z \le h_g, \\ \rho_w C_w \phi_3(z) + \rho_{mm} C_{mm}[1-\phi_3(z)], & z > h_g. \end{cases} \tag{22}$$

Details of the numerical solution of the thermal conductivity Eqs. (13) and (14) are given in the Appendix A.

The upward migration of the BHSZ with respect to its initial position is equal to $\Delta h(t) = h_g - \xi(t)$, the present-day ($t = t_p$) position is Δh_p.

3. Discussion of calculation results

The exploration drill well "METI-Nankai Trough," located approximately 20 km to the west from profile 39 of Foucher et al. (2002), indicates that the methane hydrates fill up to 40–80% of sediment pore space within a 100-m-thick layer above the BSR (Matsumoto, 2002). The measured chloride concentration varies from 100 to 560 mM and the gas hydrate saturation, obtained indirectly using the resistivity well log data, varies from 0% to 80% (Matsumoto, 2002). Both the BSR1 and the BSR2 were also observed in the vicinity of this well. Assuming that the hydrate distribution along the seismic profile is the same as at the borehole, we will assume the concentration of the hydrates (δ) to be 40% of the pore space and the thickness of the hydrate bearing layer to be 100 m. We use the sea-bottom temperature values given by Foucher et al. (2002; Fig. 8, p. 170). The depth approximations for the sea floor and both the observed BSR2 and BSR1 are taken from the same paper (Fig. 9, p. 171).

The evolution of the temperature perturbation $\delta T(h_g, t) = T(h_g, t) - T_s(h_g)$ at the initial depth of the phase boundary BSR2 for four points along profile 39 of Foucher et al. (2002) is shown on Fig. 2. Curves have

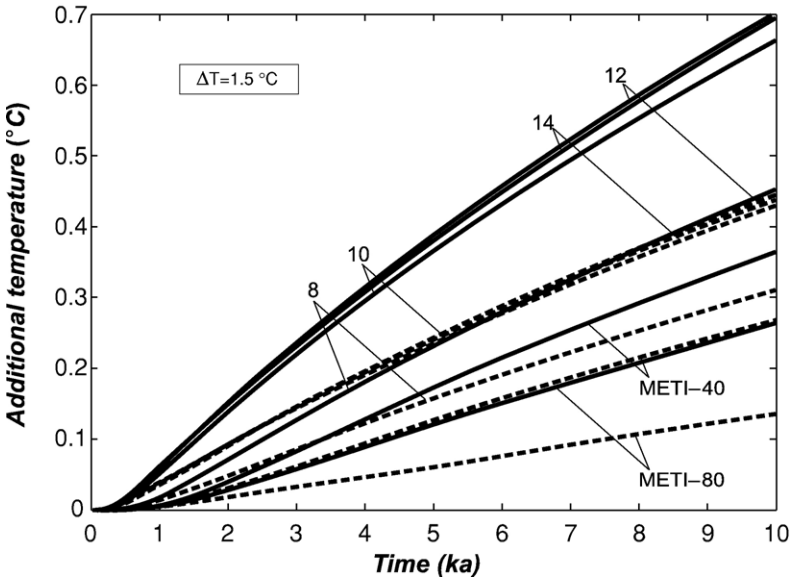

Fig. 2. Additional temperature induced by the bottom heating. Every curve corresponds to a certain point of profile 39 of Foucher et al. (2002) and takes into account the initial position of BSR2 at that point. Solid and dashed lines correspond to the methane hydrate thermal conductivities $\lambda_h = 2.1$ W m^{-1} K^{-1} and $\lambda_h = 0.6$ W m^{-1} K^{-1}, respectively. Every curve is calculated using methane hydrates concentration 40% of the pore space. The curves for the "METI-Nankai Trough" well using both $\delta = 40\%$ and $\delta = 80\%$ are also shown.

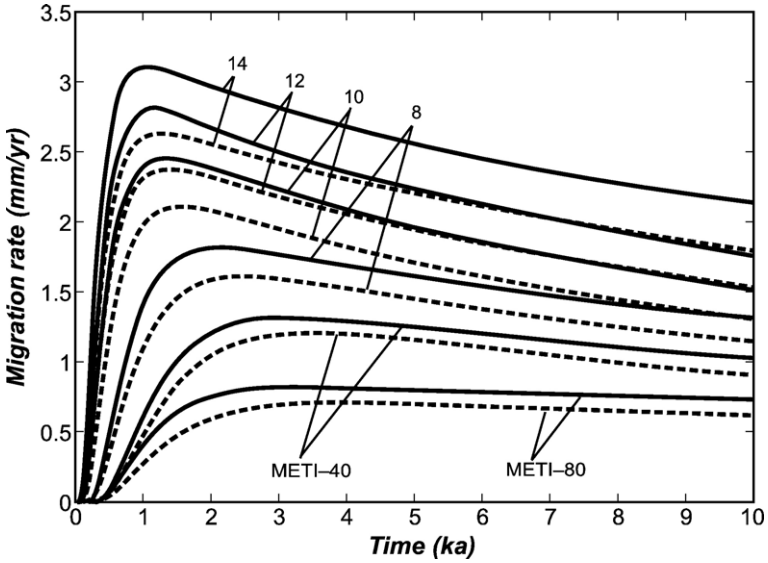

Fig. 3. Migration rate of the hydrate dissociation front. Every curve corresponds to a certain point of profile 39 of Foucher et al. (2002) and the "METI-Nankai Trough" well. Solid and dashed lines are the same as in Fig. 2.

been calculated for the following points on the profile: 8, 10, 12 and 14 km and also for the drill site. The endothermic character of the methane hydrate dissociation is evidently expressed in a two-fold reduction of the temperature change for the site near the well "METI-Nankai Trough," for the case when the hydrate concentration in the pores reaches 80% in comparison with the case for which $\delta = 40\%$.

The rate of phase boundary migration (Fig. 3) increases rapidly during the first few thousand years after the change of the bottom temperature and can reach maximum values of 1.5–3.5 mm/yr. After that the migration rate gradually decreases and at present-day it is about 70–75% of the maximum value, testifying that BHSZ is still actively moving upwards under the influence of the warming pulse of 10 ka ago. The migration rate is noticeably bigger if the hydrate thermal conductivity is larger. A similar influence of the value of the thermal conductivity on the position of the phase boundary is also marked on Fig. 4 where the history of the phase boundary migration after the change of the bottom-water temperature by 1.5 °C is demonstrated. Smaller values for the hydrate thermal conductivity lead to a smaller shift of the BHSZ.

Fig. 5 shows modeled present-day location of the BHSZ calculated for the depth section along profile 39

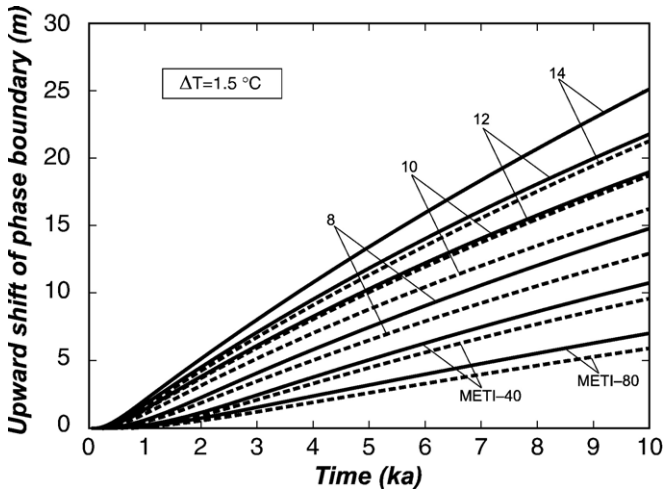

Fig. 4. History of temperature-induced upward migration of phase boundary (BSR2). Conventions of Fig. 3 are used here.

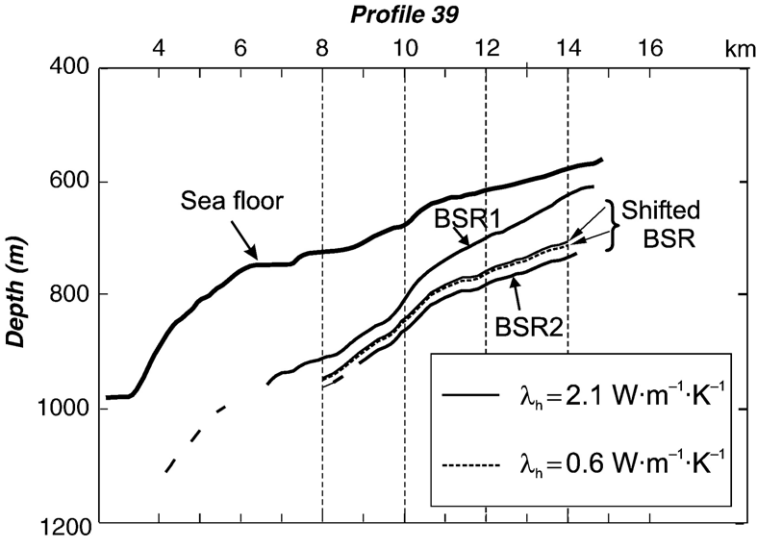

Fig. 5. Plots for the observed depths of BSR1 and BSR2 (thick solid lines) along profile 39 of Foucher et al. (2002) in comparison with the position of the phase boundary for λ_h=2.1 W m^{-1} K^{-1} (thin solid line) and λ_h=0.6 W m^{-1} K^{-1} (thin dashed line), respectively. The positions for the phase boundary were calculated by solving the Stefan problem.

of Foucher et al. (2002). It indicates the level to which the phase boundary would have been migrated from its initial position (i.e. from level of BSR2) 10 ka ago.

To estimate the reliability of the results, represented on Figs. 4 and 5, one should note the following.

The lithology of deposits below the sea floor directly influences the values of parameters such as the sediment porosity ϕ_0 near the sea-bottom, the sediment compaction parameter k and the thermal conductivity of the mineral matrix λ_{mm}. In turn the magnitude of the displacement of the phase boundary depends on the values of these parameters. If the value of the compaction parameter decreases, then the increase in the volume of gas hydrate-bearing pore space is commensurate with that, therefore an additional quantity of the thermal energy is necessary for the dissociation of the gas hydrates near the BHSZ. This leads as well to a decrease in both the thermal conductivity and the thermal diffusivity of the sediments because of the low conductivity of pore water. As a result, the upward migration of the phase boundary is slowed down. If the mineral matrix also has a low thermal conductivity this effect becomes even more noticeable. In contrast, increases in both thermal conductivity of the mineral matrix and the compaction parameter intensifies the upward migration of the phase boundary.

Data from the "METI-Nankai Trough" exploration well show that the uppermost 100 m of sediments are mudstones–siltstones with sporadic ash beds. Below them is mudstone with an increasing number of sandstone beds towards the BHSZ. Gas hydrate is pure methane hydrate (Foucher et al., 2002; Matsumoto, 2002). It partly fills the pore-space of sandy and silty layers (Matsumoto, 2002).

The near-bottom porosity ϕ_0 of argillaceous and sandy sediments lies in the range of 0.56–0.63 and has an average of 0.6 (Sclater and Cristie, 1980; Hutchison, 1985). The compaction parameter k for a shale varies from 0.51 (Sclater and Cristie, 1980) to 0.65 km^{-1} (Hutchison, 1985). For sandstones the same authors suggest the following range for this coefficient: 0.27 km^{-1} ≤ k ≤ 0.36 km^{-1}. For shaley sandstones the average value of the compaction parameter is k ≈ 0.4 km^{-1} (Sclater and Cristie, 1980). The thermal conductivity of minerals common in terrigenous sediments ranges mainly between 1.5 and 2.6 W m^{-1} K^{-1} (Allen and Allen, 2005).

Taking these data into account we have chosen two pairs of extreme values for these parameters: (1) k = 0.3 km^{-1}, λ_{mm} = 1.5 W m^{-1} K^{-1}; (2) k=0.65 km^{-1}, λ_{mm}=2.6 W m^{-1} K^{-1}. The first provides the minimal displacement of the phase boundary, while the second provides the maximum.

All our calculations, the results of which are shown in Figs. 2 3 4 and 5, were performed using the following values which are typical of the upper part of the normal sedimentary sequence below the ocean floor: ϕ_0=0.6, k=0.45 km^{-1}, λ_{mm}=2.1 W m^{-1} K^{-1}.

To estimate the potential influence of the lithology on the magnitude of the displacement of the phase boundary

we carried out special calculations for selected points along profile 39 of Foucher et al. (2002) and the "METI-Nankai Trough" borehole. Calculations for each of these points were performed using both pairs of extreme values, first using a value of 0.6 W m^{-1} K^{-1} for λ_h, the thermal conductivity of the methane hydrate, and second using λ_h=2.1 W m^{-1} K^{-1}. As a result possible extreme migration magnitudes, Δh_{ex}, of the BHSZ were estimated.

For calculations of the bulk thermal conductivity of the three-component sediment consisting of mineral grains, pore water and methane hydrate, the model of the effective randomly inhomogeneous medium (Allen and Allen, 2005) was used. Within the framework of this model the thermal conductivity, $\tilde{\lambda}_2$, of the second layer was determined by solving the following cubic equation:

$$\frac{1}{\tilde{\lambda}_2} = 3\left[\frac{1-\tilde{\phi}}{2\tilde{\lambda}_2+\lambda_{mm}} + \frac{(1-\delta)\tilde{\phi}}{2\tilde{\lambda}_2+\lambda_w} + \frac{\tilde{\phi}\delta}{2\tilde{\lambda}_2+\lambda_h}\right].$$

One should note that the dependence (8) is a particular case of the model of the effective medium for a two-component sediment.

We used the maximal absolute difference δh between the extreme Δh_{ex} and normal Δh_p BHSZ migration magnitudes as a measure of the influence of the lithology.

The values of both the normal and the extreme upward migration of the phase boundary and also the measure of the difference between them are given in Table 1. It is obvious that the value of δh could be considered as a measure of the reliability of the results presented in Figs. 4 and 5.

As seen from Fig. 5 and Table 1, present-day displacement of the phase boundary calculated using our model are appreciably less than the actual differences d between BSR2 and BSR1 depths for all points of profile 39 (of Foucher et al., 2002) and for "METI-Nankai Trough" (Matsumoto, 2002).

To estimate the influence of the methane hydrate concentration in the sediment pore space on the displacement magnitude, we carried out an additional study at a single point ("10 km") along the profile. The calculations cover the whole range of hydrate concentration from 0% to 100% of the total pore space (Appendix B).

Fig. 6 shows the dependence of today's BSR depth Δh_p on the relative methane hydrate volume in the pore

Table 1
Results of calculations of the phase boundary displacement at the present time Δh_p and Δh_{ex}

Point		h_w (m)	z_{BSR1} (mbsf)	z_{BSR2} (mbsf)	T_w (°C)	ΔT (°C)	T_w^0 (°C)	d (m)	λ_h (W m^{-1} K^{-1})	λ_{mm} (W m^{-1} K^{-1})	k (km^{-1})	Δh_{ex} (m)	$\Delta h_p \pm \delta h$ (m)
Borehole	δ=40%	945	270	300	3.7	1.5	2.2	30	2.1	1.5	0.3	8.9	10.7±1.8
METI-Nankai										2.6	0.65	12.4	
Trough									0.6	1.5	0.3	7.9	9.6±1.7
										2.6	0.65	11.1	
	δ=80%	945	270	300	3.7	1.5	2.2	30	2.1	1.5	0.3	5.8	7.0±1.2
										2.6	0.65	8.2	
									0.6	1.5	0.3	4.8	5.9±1.1
										2.6	0.65	7.0	
Profile 39	8 km	725	190	240	4.4	1.5	2.9	50	2.1	1.5	0.3	12.5	14.8±2.3
δ=40%										2.6	0.65	16.8	
									0.6	1.5	0.3	10.9	12.9±2
										2.6	0.65	14.6	
	10 km	680	130	185	4.8	1.5	3.3	55	2.1	1.5	0.3	16.5	19.0±2.4
										2.6	0.65	21.0	
									0.6	1.5	0.3	14.2	16.2±2
										2.6	0.65	17.9	
	12 km	625	90	170	5	1.5	3.5	80	2.1	1.5	0.3	19.0	21.8±2.8
										2.6	0.65	24.0	
									0.6	1.5	0.3	16.3	18.7±2.4
										2.6	0.65	20.6	
	14 km	580	50	160	5.3	1.5	3.8	110	2.1	1.5	0.3	21.8	25.1±3.3
										2.6	0.65	27.8	
									0.6	1.5	0.3	18.5	21.2±2.7
										2.6	0.65	23.3	

Here $d=z_{BSR2}-z_{BSR1}$.

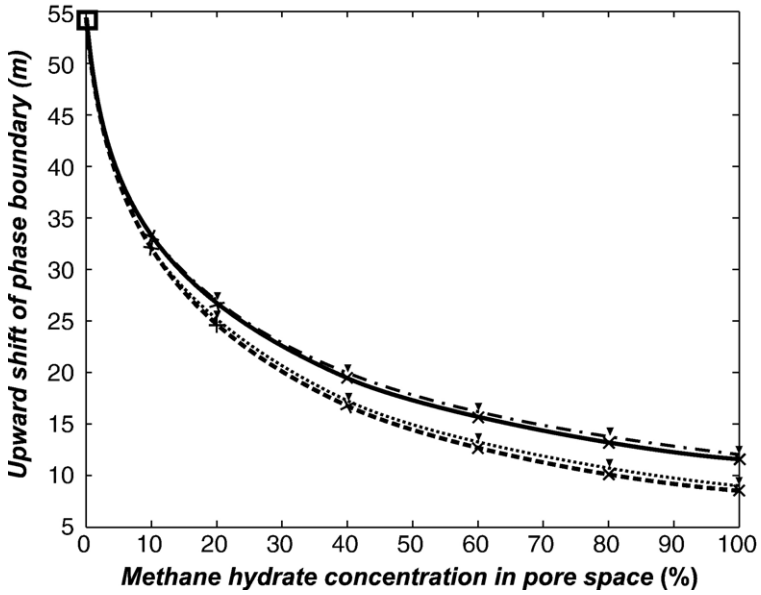

Fig. 6. Upward shift of the phase boundary (BSR2) as a function of methane hydrate concentration, δ, in the pores. Computations were carried out with conditions for point "10 km" of profile 39 of Foucher et al. (2002). Solid and dashed lines correspond to the thermal conductivity of the methane hydrate of λ_h=2.1 W m^{-1} K^{-1} and λ_h=0.6 W m^{-1} K^{-1}, respectively, when a porosity in the methane hydrate-bearing layer is constant. Crosses mark the calculated values. Dash dotted and dotted lines correspond to the same values of the thermal conductivity if a porosity in such a layer is non-constant and varies with depth according to Athy's law (Athy, 1930). In this case the calculated values are marked by black triangles. Asymptotic value for δ=0 is shown with a small square.

space (δ). It can clearly be seen that an increase in the hydrate concentration leads to a decrease in the present-day phase boundary migration, which is explained by additional thermal energy consumption for the endothermic reaction of the dissociation. It demonstrates also that only in case of total absence of the gas hydrates, i.e. $\delta \rightarrow 0$, is our calculated depth similar to the observed difference between depths of the BSR2 and the BSR1 (Foucher et al., 2002).

If the porosity in the gas-hydrate-bearing layer would decrease with depth as in the hydrate-free sediment cover, the relative amount of the methane hydrate in the sediments close to the BHSZ should be smaller than in the case which we examine here, when the porosity in this layer is constant and equal to its value on the layer's top. It would lead to the decrease in the thermal energy consumption for the dissociation of the gas hydrates and the upward shift of the phase boundary should be therefore increased. It is equivalent to the lowering of the methane hydrate concentration in the pore space of sediments with a constant porosity. This effect can be seen on Fig. 6 where the dotted and the dash-dotted lines show how our calculated magnitude of the upward shift of the BHSZ depends on the hydrate concentration in the pore space of sediments if their porosity varies with depth according to Athy's law (Athy, 1930), where parameters are of typical above-mentioned values. However, as it appears from Fig. 6, the magnitudes of the upward migration of the phase boundary differ insignificantly in both these cases.

One may infer from the above that the sudden 1.5 °C increase in sea-bottom temperature that happened about 10 ka ago was insufficient to displace the phase boundary upwards from BSR2 to BSR1.

To estimate the increase in sea-bottom temperature that would have been required to move the BHSZ from the first level to the second, we performed special calculations for each selected point along profile 39 of Foucher et al. (2002) and the "METI-Nankai Trough" borehole.

Fig. 7 represents the present-day displacement of the phase boundary, Δh_p, as the dependence on the amplitude of the sea-bottom temperature rise ΔT. It appears from this figure that if the hydrate concentration in pores is equal to δ=40% then to move the phase boundary upward by the necessary distance it would be necessary to increase the sea-bottom temperature by either 4.4–5.2 °C, when the thermal conductivity of the hydrate is equal to λ_h=0.6 W m^{-1} K^{-1}, or 3.9 to 4.6 °C if λ_h=2.1 W m^{-1} K^{-1}. If the hydrate concentration is equal to δ=80% the bottom-water should be warmed by either 7.2 or 6 °C respectively.

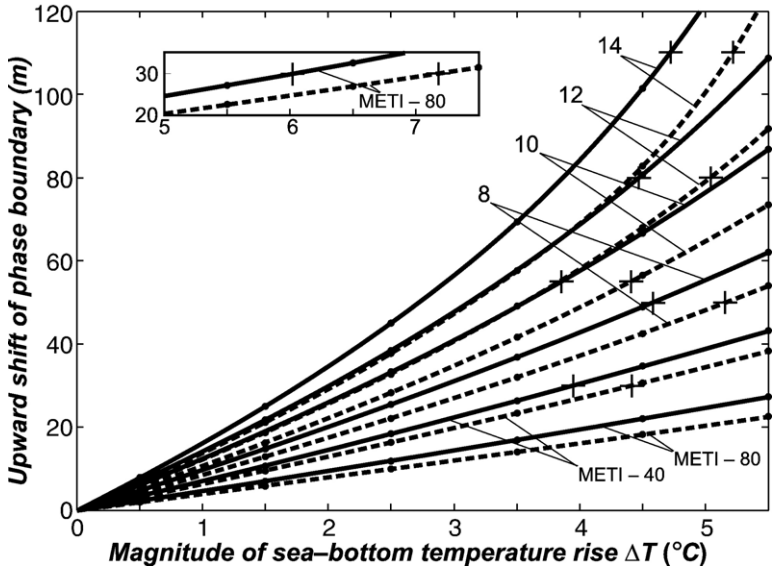

Fig. 7. Upward shift of the phase boundary (BSR2) as a dependence on an amplitude of sea-bottom temperature rise, ΔT. Every curve corresponds to a certain point of profile 39 of Foucher et al. (2002) and the "METI-Nankai Trough" well when methane hydrate concentration is equal to δ=40% of the pore space. The curve for the "METI-Nankai Trough" well with δ=80% is also shown in the inset. Solid and dashed lines correspond to the methane hydrate thermal conductivities λ_h=2.1 W m^{-1} K^{-1} and λ_h=0.6 W m^{-1} K^{-1}, respectively. Solid circles mark the computed values, crosses specify the temperature step amplitudes, which correspond with observed differences between depths of the BSR2 and the BSR1.

One should note that the computed required sea-bottom temperature rise practically coincides with the rise in surface water temperature of the Kuroshio over the last 18 ka, as reported by Sawada and Handa (1998). However, it is difficult to imagine that a similar rise in water temperature would occur also at the depth of the sea floor.

4. Conclusions

Considering the model that takes into account the latent heat of hydrate dissociation, we showed that: (1) the latent heat is the controlling factor in the phase boundary displacement value; and (2) the double BSR in the Nankai Trough could appear as a result of the displacement of the hydrate phase boundary, caused by an abrupt increase of the sea-bottom temperature, only if the value of this thermal impact was equal to approximately 4 °C or more. Moreover, taking into account the fact that hydrates do not necessarily fill only the existing pores and cavities, as assumed in our model, but can occupy extra space by the formation of massive hydrate bodies, the rate of hydrate dissociation (or the rate of upward migration of the phase boundary) can become even less and a much greater sea-bottom temperature warming is not very probable in the Nankai Trough. At last, here we examine only how the increase in the bottom-water temperature could result in the upward migration of the BHSZ, and therefore we do not take into account the influence of the post-glacial rise in sea level, and thus the pressure rise, which would have a counteracting effect on the warming pulse and should decrease the upward shift of the phase boundary. Consequently the paleooceanographic interpretation of the nature of the double BSR does not appear to be reliable enough.

On the other hand, the obtained results may also indicate that in the past the gas hydrates were absent within the most part of the layer between present-day reflectors BSR1 and BSR2.

If it is assumed that the free gas below the BSR2 level is in sufficient quantity to support the necessary reflectivity of this boundary today even after the upward migration of the stability zone base, then we would favour a tectonic rather than a thermal nature of the double BSR.

At the same time there is reason to suggest that the BSR2 is not a hydrate-related BSR. In particular, it may be the free gas released from gas-bearing water that moves towards the sea floor. By the way, the fact, that the BSR2 is parallel to the sea floor whereas the BSR1, that is the shallower boundary, dips more steeply, can indirectly testify that only one of these reflections is hydrate-related BSR.

In order to explain the nature of double or multiple BSRs, we believe it is necessary to examine and other factors apart from paleooceanographic ones, for example, lithological and geochemical features of the sedimentary cover.

Acknowledgements

The authors would like to thank Ross Chapman, Michael Zykov of University of Victoria, Canada, Roy Hyndman of Geological Survey of Canada (Pacific Geoscience Centre), John Woodside of Free University of Amsterdam, Netherlands, Alan Judd of University of Sunderland, England, and Jeffrey Poort of University of Gent, Belgium, for very constructive discussion of our results and for the improvement of our English. We are especially grateful to Mark de Batist of University of Gent, Belgium, for his thorough analysis of our work and very valuable advices on how to improve both the contents and the language of this paper.

Appendix A

The thermal conductivity Eqs. (13) and (14) are numerically solved using the finite-difference method and taking into account the continuity of heat flow at any point of sediment layer. The resulting system of the linear algebraic equations for the discrete values of the temperature is given by:

$$A_k \cdot T_{k-1,j} - C_k \cdot T_{k,j} + B_k \cdot T_{k+1,j} = -F_k. \tag{A1}$$

Here:

$$\begin{aligned}
&T_{k,j} = \begin{cases} T^-(z_k, t_j), & 0 \le z_k \le \xi(t_j), \quad 1 \le k \le N_1, \\ T^+(z_k, t_j), & z_k \ge \xi(t_j), \quad 1 \le k \le N_2 \end{cases} \\
&A_k = \frac{a_k \tau / h^2}{1 + \frac{\lambda_{k+1}}{\lambda_k} \cdot \frac{a_k}{a_{k+1}}} \\
&B_k = \frac{\lambda_{k+1}}{\lambda_k} A_k; \\
&C_k = 1 + A_k + B_k; \\
&W_k = 1 - A_k - B_k; \\
&F_k = A_k \cdot T_{k-1,j-1} + W_k T_{k,j-1} + B_k \cdot T_{k+1,j-1};
\end{aligned} \tag{A2}$$

$\lambda_k = \lambda(z_k)$ is the thermal conductivity determined by formulas (19), (20); $a_k = a(z_k) = \lambda(z_k)/\overline{\rho C}(z_k)$ is the thermal diffusivity when the specific heat, $\overline{\rho C}(z_k)$, is determined by formulas (21), (22); $h = z_k - z_{k-1}$ is constant grid spacing that is different for each $t = t_j$ and in different areas $z \le \xi(t_j)$ and $z > \xi(t_j)$; N_1 is the constant number of the spatial grid points in the first of these areas and N_2 is the same in the second one; $\tau = t_j - t_{j-1}$ is the constant time step.

In addition, the following boundary and initial conditions are used:

1) upper area, $0 = z_1 \le z_k \le z_{N_1} = \xi(t_j)$,

$$T_{1,j} = T_w^0 + \Delta T, \quad T_{N_1,j} = T_{ph}(\xi(t_j)), \quad T_{k,0} = T_s(z_k); \tag{A3}$$

2) lower area $\xi(t_j) = z_1 \le z_k \le z_{N_2} = H$,

$$T_{1,j} = T_{ph}(\xi(t_j)), \quad T_{N_2,j} = T_s(H), \quad T_{k,0} = T_s(z_k). \tag{A4}$$

The obtained systems of linear Eqs. (A1) together with mentioned conditions (A3), (A4) are solved by the double-sweep method. The discrete version (A1) of Eqs. (13) and (14) should be solved with high accuracy in order to have the reliable values of the temperature gradients included in Eq. (11). It is achieved by choosing the appropriate value for the numbers of the spatial grid points and the time step.

Appendix B

The way that was described above cannot be solved for the displacement for the case when $\delta \to 0$ since in the right part of the Eq. (11) both numerator and denominator approaches zero. In order to obtain the solution, it is necessary to take into account the fact that in case the sedimentary cover does not contain the methane hydrates then the temperature of sediment is the sum of the stationary geotherm $T_s(z)$ and the perturbation $\tilde{T}(z, t)$ caused by seafloor temperature's jump by ΔT at time $t = 0$. We used the intersection of the present-day temperature vertical profile with the methane hydrate stability curve to evaluate the quantity in question. The temperature perturbation $\tilde{T}(z, t)$ in the depth range $0 \le z \le H$ is the solution of the thermal conductivity equation similar to Eq. (13) but with the following boundary and initial conditions:

$$\tilde{T}(0, t) = \Delta T, \quad \tilde{T}(H, t) = 0, \quad \tilde{T}(z, 0) = 0.$$

The method of the numerical solution of this equation was given in Appendix A.

References

Allen, P.A., Allen, J.R., 2005. Basin Analysis: Principles and Applications, second edition. Blackwell Sci. Publ., Oxford. 549 pp.

Athy, L.F., 1930. Density, porosity and compaction of sedimentary rocks. Am. Assoc. Pet. Geol. Bull. 14, 1–24.

Bangs, N.L.B., Musgrave, R.J., Tréhu, A.M., 2005. Upward shifts in the southern Hydrate Ridge gas hydrate stability zone following postglacial warming, offshore Oregon. J. Geophys. Res. 110, B03102. doi:10.1029/2004JB003293.

Berndt, C., Bünz, S., Clayton, T., Mienert, J., Sounders, M., 2004. Seismic character of bottom simulating reflectors: examples from the mid-Norwegian margin. Mar. Pet. Geol. 21, 723–733.

Budiansky, B., 1970. Thermal and thermoelastic properties of isotropic composites. J. Compos. Mater. 4, 286–295.

Clauser, C., Huenges, E., 1995. Thermal conductivity of rocks and minerals. In: Ahrens, T.J. (Ed.), Rock Physics and Phase Relations: a Handbook of Physical Constants. AGU, Washington, pp. 105–126.

Domenico, S.N., 1976. Effect of brine-gas on velocities in an unconsolidated sand reservoir. Geophysics 41, 882–894.

Foucher, J.-P., Nouze, H., Henry, P., 2002. Observation and tentative interpretation of a double BSR on the Nankai slope. Mar. Geol. 187, 161–175.

Ginsburg, G.D., Soloviev, V.A., 1994. Submarine gas hydrates. All-Russia Research Institute for Geology and Mineral Resources of the World Ocean "VniiOkeangeologiya", St. Petersburg. 199 pp.

Golmshtok, A.Ya., 2003. Variations in bottom temperature and stability conditions of gas hydrates [in Russian]. Russ. J. Geophys. 31–32, 23–36.

Groisman, A.G., 1985. Thermophysical Properties of Gas Hydrates [in Russian]. Nauka, Novosibirsk. 94 pp.

Hutchison, I., 1985. The effects of sedimentation and compaction on oceanic heat flow. Geophys. J. R. Astron. Soc. 82, 439–459.

Istomin, V.A., 1999. Phase Equilibrium and Physical–Chemical Properties of Gas Hydrates [in Russian]. Gazprom, Moscow. 41 pp.

Matsumoto, R., 2002. Comparison of Marine and Permafrost Gas Hydrates: Examples from Nankai Trough and Mackenzie Delta. Proceedings of the Fourth International Conference on Gas Hydrates, Yokohama, May 19–23, 2002, pp. 1–5.

Miller, J.J., Lee, M.W., von Huene, R., 1991. An analysis of a seismic reflection from the base of a gas hydrate zone, offshore Peru. Am. Assoc. Pet. Geol. Bull. 75 (5), 910–924.

Murphy, W.F., 1984. Acoustic measures of partial gas saturation in tight sandstone. J. Geophys. Res. 89, 11549–11559.

Ozerskaya, M.L., Tuyezova, N.A., 1984. Density and porosity of sedimentary rocks. In: Dortman, N.B. (Ed.), Physical Properties of Rocks and Minerals. (Petrophysics). Reference Book for Geophysicists [in Russian]. Nedra, Moscow, pp. 65–77.

Popescu, I., Lericolais, G., De Batist, M., Panin, N., 2003. Characteristic of the gas charged sediments in the north-western Black Sea. Ocean Margin Research Conference. Abstract volume. UNESCO, Paris.

Posevang, J., Mienert, J., 1999. The enigma of double BSRs: indicators for changes in the hydrate stability field. Geo-Mar. Lett. 19, 157–163.

Sawada, K., Handa, N., 1998. Variability of the path of the Kuroshio ocean current over the past 25000 years. Nature 392, 592–594.

Sclater, J.G., Cristie, P.A.F., 1980. Continental stretching: an explanation of the post Mid-Cretaceous subsidence of the central North Sea basin. J. Geophys. Res. 85, 3711–3739.

Selim, M.S., Sloan, E.D., 1990. Hydrate dissociation in sediment. SPE Reserv. Eng. 5, 249–251.

Shipley, T.H., Houston, M.H., Buffler, R.T., et al., 1979. Seismic reflection evidence for the widespread occurrence of possible gas-hydrates horizons on continental slopes and rise. AAPG Bull. 63 (12), 2204–2213.

Sloan, E.D., 1990. Clathrate Hydrates of Natural Gases. Marcel Dekker Inc., NY. 641 pp.

Sloan, E.D., 1996. The Colorado School of Mines Hydrate Prediction Program (CSMHYD). Centre for Hydrate Research, Colorado School of Mines.

Sultan, N., Foucher, J.P., Cochonat, P., Tonnerre, T., Bourillet, J.F., Ondreas, H., Cauquil, E., Grauls, D., 2004. Dynamics of gas hydrate: case of the Congo continental slope. Mar. Geol. 206, 1–18.

Taylor, A.E., Dallimore, S.R., Hyndman, R.D., Wright, F., 2002. Comparing the sensitivity of terrestrial and marine gas hydrates to climate warming at the end of the Last Ice Age. Proceedings of the Fourth International Conference on Gas Hydrates, Yokohama, May 19–23, 2002, pp. 63–70.

Tucholke, B.J., Bryan, G.M., Ewing, J.I., 1977. Gas-hydrates horizons detected in seismic-profiler data from the Western North Atlantic. Am. Assoc. Pet. Geol. Bull. 61 (5), 698–707.

Waite, W.F., deMartin, B.J., Kirby, S.H., Pinkston, J., Ruppel, C.D., 2002. Thermal conductivity measurements in porous mixtures of methane hydrate and quartz sand. Geophys. Res. Lett. 29 (24), 2229. doi:10.1029/2002GL015988.

Yamano, M., Uyeda, S., Aoki, Y., et al., 1982. Estimates of heat flow derived from gas hydrates. Geology 10 (7), 339–343.